AD-A207 656 MORPHOLOGY AND CHEMICAL PROPERTIES OF THE DOW PERFLUOROSULFONATE IONOMERS(U) TEXAS A AND M UNIV COLLEGE STATION DEPT OF CHEMISTRY R B MOORE ET AL. 1/1

UNCLASSIFIED 1988 N00014-82-K-0612 F/G 7/6 NL

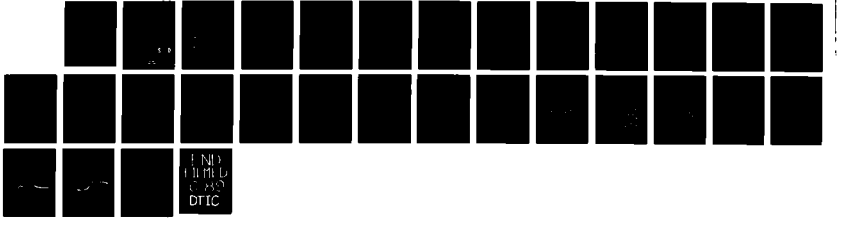

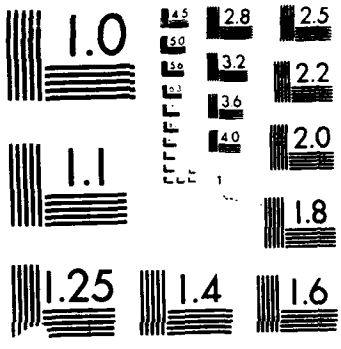
1.0
1.1
1.25
1.4
1.6
1.8
2.0
2.2
2.5
2.8
3.2
3.6
4.0
4.5
5.0
5.6

Contract N00014-82-K-0612

Morphology and Chemical Properties of the Dow Perfluorosulfonate Ionomers

Robert B. Moore, III[1] and Charles R. Martin*
Department of Chemistry
Texas A&M University
College Station, Texas 77843

[1]Current Address: Department of Chemistry
McGill University
801 Sherbrooke Street West
Montreal, Quebec, Canada H3A 2K6

ABSTRACT

The Dow Chemical Company has developed an interesting new class of perfluorosulfonate ionomers (PFSI's). We have conducted a broad-based investigation of the supermolecular structures of these PFSI's. Small-angle x-ray scattering data showed that the Dow PFSI's contain ionic clusters. The sizes of these clusters vary with equivalent weight and water content. Wide-angle x-ray diffraction and differential scanning calorimetry demonstrated that PFSI's with equivalent weights greater than ca. 800 g/mole are partially crystalline. The extent of crystallinity increases with equivalent weight. Surprisingly, the melting point of the Dow PFSI's varied only slightly with equivalent weight. This suggests that these are block-type copolymers. We have also developed dissolution and solution-casting procedures for a wide range of equivalent weights of these PFSI's.

INTRODUCTION

Perfluorosulfonate ionomers (PFSI's) are cation-conducting polymers with good chemical and thermal stabilities (1-4). These polymers have been used in a variety of electrochemical processes and devices including chlor-alkali cells (3,4), fuel cells (5), water electrolyzers (6), and polymer-modified electrodes (7-12). The Nafion^R polymers (Du Pont, structure I) have been the most extensively studied PFSI's.

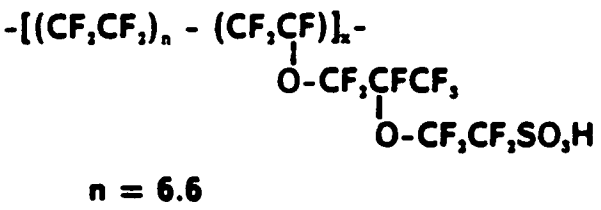

I

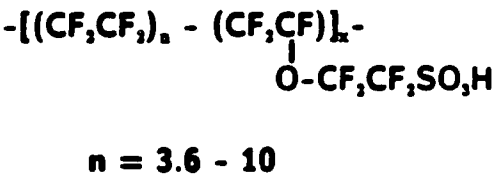

II

Recently, the Dow Chemical Company has developed a new class of PFSI's (2,4). The Dow PFSI's (structure II) contain a shorter side chain than the Nafion polymers. We have obtained samples of various equivalent weights (EW's) of the Dow polymers and we are evaluating the performances of these polymers in fuel cell applications (13,14). In support of this work, we have conducted fundamental investigations of the solubilities and the chemical and morphological properties of the Dow PFSI's. We report the results of these and related investigations here.

EXPERIMENTAL SECTION

Materials. H^+-form PFSI membranes, having EW's of 635, 803, 909, 1076 and 1269 g/(mole of $-SO_3^-$ sites), were obtained from the Dow Chemical Company. The as-received membranes were refluxed in 8M HNO_3 (for ca. 24 hours) to remove discoloring impurities. The membranes were then converted to the

Na^+-form by soaking overnight in 1M NaOH. Excess NaOH was removed by thoroughly rinsing the membranes with purified water. Ag^+-form PFSI was prepared by soaking the membranes in 1M $AgNO_3$ for 24 hours. Quenched Na^+-form PFSI samples were prepared by heating the membranes, in a muffle furnace (350°C), and then rapidly cooling in liquid N_2.

Instrumental Methods. The wide-angle X-ray diffraction (WAXD) studies were conducted on dry, Na^+-form membranes (15). Differential scanning calorimetry (DSC) data were obtained as described previously (15). Small-angle X-ray scattering (SAXS) experiments were performed using the Oak Ridge National Laboratory 10 meter SAXS system with a 2 dimensional position-sensitive proportional counter. The rotating anode x-ray source was operated at 40 kV and 60 mA. SAXS analyses were performed on hydrated, Na^+-form and dry, Ag^+-form PFSI membranes. The Na^+-form PFSI samples were hydrated by boiling in water for 1 hour. The Ag^+-form PFSI samples were dried in a vacuum oven for 12 hours at 125°C. The SAXS data were analyzed as described previously (15).

Dissolution Procedures. A high temperature procedure for dissolving the Nafion polymers was developed in these laboratories (16). The dissolution procedures, developed here, for the Dow PFSI's are similar to the Nafion process; however, the solvent and temperature needed to dissolve the Dow PFSI's varied with EW of the polymer. Table I outlines the specific dissolution conditions required for each EW of the Dow polymers.

Film-Casting Procedures. We have shown that the quality and solubility of solution-cast Nafion films are highly dependent on the solvent and temperature used during film-formation (15). Analogous effects were

observed for the Dow PFSI's investigated here. The following film-casting procedures were developed for these polymers: In a 30 mL beaker, 2 mL of dimethylsulfoxide (DMSO) were added to 5 mL of a 1 (w/v) % PFSI solution. The resulting solution was heated, in an oil bath at ca. 95°C, to remove the original alcohol-water solvent. Finally, the solution-cast film was formed by evaporating the resulting DMSO solution of the PFSI to dryness at an elevated temperature (Figure 7). Solution-cast films of the 1269 EW PFSI were also prepared from triethyl phosphate and propylene carbonate solutions. Film quality was assessed by determining the solubility of the solution-cast film in room temperature ethanol/water (15).

RESULTS AND DISCUSSION

Wide-Angle X-Ray Diffraction. Figure 1 shows WAXD data for five EW's of the Dow PFSI's. A distinct crystalline scattering peak at ca. 18°, 2θ is observed for the higher EW polymers. Since this peak occurs at the same angle as the crystalline scattering peak in Teflon (15), this reflection is attributed to Teflon-like crystallinity in the PFSI. A similar reflection is observed from the Nafion polymers (15).

Since the integrated intensity of the crystalline peak (relative to the amorphous halo) is a measure of the extent of crystallinity (17), it is clear that the extent of crystallinity increases with EW; Gierke et al. observed a similar trend for Nafion (18). The dependence of crystallinity on EW is attributed to the disruptive effect of the side chains on the lamellar ordering of the tetrafluoroethylene backbone segments (19). As EW increases the quantity of side chains decreases, and thus more of the polymer is able to crystallize (18).

Figure 2 compares WAXD data for 1100 EW Nafion (curve A), 909 EW Dow PFSI (curve B) and 1076 EW Dow PFSI (curve C). The crystalline peak for Nafion appears as a shoulder on the amorphous halo. In contrast, a distinct peak is observed in the lower EW Dow polymer (curve B). Clearly, the Dow PFSI's are more crystalline than the Nafion polymers. Higher crystallinity results because the shorter Dow side chain disrupts backbone chain crystallization to a lesser extent than does the longer Nafion side chain.

Differential Scanning Calorimetry. Figure 3 shows thermograms for the Dow PFSI's. Depending on EW, either two or three endotherms are observed. We have assigned the first endotherm (150 to 180° C), to the matrix glass transition ($T_{g,m}$) (15). The second endotherm (270 to 300° C) is assigned to the ionic cluster glass transitions ($T_{g,c}$) (15). The higher EW polymers show a third endotherm (ca. 335° C). We have assigned this endotherm to the melting of the PFSI crystals (T_m). Table II lists the temperatures of these transitions. The reasons for making these assignments are presented below.

DSC and dynamic mechanical analyses have shown that the matrix glass transition of Na^+-form Nafion occurs at ca. 150° C (20,21). Since the Dow PFSI s show the classical step-shaped increase in the rate of heat consumption near the $T_{g,m}$ of Nafion, the endotherms between 150 and 180° C were attributed to the matrix glass transitions. Side chains can act as plasticizers and lower the glass transition temperatures of polymeric systems (22). Furthermore, longer side chains have a stronger plasticizing effect than shorter side chains (22). Thus, we propose that Nafion has a lower $T_{g,m}$ than the Dow PFSI's because Nafion has a longer side chain.

The matrix glass transition temperatures for the Dow PFSI's increase with decreasing EW (Table II); this effect is commonly observed in ionomers

and has been attributed to the formation of electrostatic crosslinks (23). These crosslinks result from aggregation of the ionic groups and diminish the mobility of the polymer backbone chain. Since ionic aggregation increases with decreasing EW (18), the lower EW polymers are more highly crosslinked and yield higher $T_{g,m}$'s.

Na^+-form Nafion shows a dynamic mechanical analysis relaxation at ca. 240° C (21). Eisenberg attributes this relaxation to the ionic cluster glass transition ($T_{g,c}$) (21). We have shown that this relaxation appears as a broad endothermic peak in the DSC thermograms of 1100 EW Nafion (15). While the shape of this endotherm is unusual for a glass transition (i.e., a peak as opposed to a step), the assignment of this peak as the $T_{g,c}$ was supported by the fact that the position of this peak was counterion-dependent (15).

The positions of the $T_{g,c}$ peaks in the Dow PFSI's are also counterion dependent. For example, in the Na^+-form 1086 EW polymer this peak occurs at 286°C; the peak shifts to 305° C in the Mn^{2+}-form polymer. Furthermore, because this endotherm is observed in the noncrystalline 635 EW polymer (Figure 3), this transition cannot originate from the crystalline phase. For these reasons, we have assigned the 270 to 300° C endotherm to the glass transition of the ionic clusters in the Dow PFSI's. The higher $T_{g,c}$ of the Dow polymers, relative to Nafion, may be attributed to the plasticization effect of water within the clusters (20); because the Dow PFSI's imbibe less water (4), the Dow $T_{g,c}$'s occur at higher temperatures.

The lower EW PFSI's show higher $T_{g,c}$'s than the higher EW polymers (Table II). Eisenberg et al. observed a similar effect in styrene ionomers (24,25). As discussed in our previous paper (15), as the concentration of

sulfonate sites increases (decreasing EW), the electrostatic interactions in the ionic clusters increase, and thus $T_{g,c}$ is elevated.

The third (ca. 335° C) endotherm is apparently unique to the Dow PFSI's. This high temperature peak is not observed in the thermogram of the noncrystalline 635 EW polymer (Figure 3). Furthermore, this endotherm is not observed in quenched (and thus noncrystalline) samples of the Dow polymers. Finally, this high temperature peak occurs at nearly the same temperature as the melting temperature of virgin polytetrafluoroethylene (26). For these reasons, we have assigned this high temperature endotherm to the melting (T_m) of the PFSI crystalline regions.

The heat of fusion (ΔH_f) can be calculated from the area under the T_m peaks in Figure 3; ΔH_f is proportional to the extent of crystallinity in the polymer (27). The ΔH_f values for the Dow PFSI's increase from 0.02 cal/g for the 803 EW polymer to 1.46 cal/g for the 1269 EW polymer. In agreement with the WAXD data (Figure 1), these data demonstrate that crystallinity in the Dow PFSI's increases with EW.

Assuming (for the moment) that the Dow PFSI's are random copolymers, the crystalline melting point, for any EW, may be calculated via (28)

$$1/T_m - 1/T_m^o = -(R/\Delta H_m)\ln n \qquad (1)$$

where T_m^o is the melting point of the analogous homopolymer (polytetrafluoroethylene), T_m is the melting point of the copolymer, R is the gas constant, ΔH_m is the heat of fusion per mole of crystallizable units, and *n* is the mole fraction of crystallizable units. Equation 1, predicts that T_m for the 909 EW PFSI should be 13° C lower than T_m for the 1076 EW polymer; only a 2° C decrease in T_m is observed experimentally

(Table II). Note further that the T_m values for the PFSI's (Table II) are essentially identical to T_m for the homopolymer (26).

Okuda obtained analogous data for vinylidene chloride/vinyl chloride copolymers (29). At comonomer ratios similar to those studied here, the vinylidene chloride/vinylchloride copolymers showed melting points very similar to that of polyvinylidine chloride homopolymer. Furthermore, a morphological investigation of the copolymers showed that the crystalline vinylidine chloride sequences were much longer than would be predicted based on a random model (29). Thus, Okuda concluded that vinylidine chloride-vinyl chloride was a block, rather than a random, copolymer (29).

The similarity between the PFSI and the vinylidine chloride-vinylchloride data suggests that the Dow PFSI's are not random copolymers. We suggest that the Dow polymers contain blocks of tetrafluoroethylene units which are larger than would be expected assuming a purely random distribution of monomers. The crystallites form from these long tetrafluoroethylene blocks. The amorphous regions contain shorter tetrafluoroethylene sequences and the perfluoroether side chains.

The increase in crystallinity with EW (Figures 1 and 3) is consistent with this block-type model. As EW increases, the quantity of perfluoroether comonomer decreases. This decrease in comonomer content increases the average tetrafluoroethylene block length, which increases the number of blocks of sufficient length to form crystals.

Water Content. Figure 4 shows that the water content of the 635 EW PFSI is significantly higher than the water contents of the other polymers. The 635 EW polymer imbibes more water because it is not crystalline. This conclusion is corroborated by a comparison of the water contents of as-received and

quenched PFSI's. As-received 909 EW PFSI absorbs ca. 25 percent water by weight; however, when the crystallinity is removed by quenching, the 909 EW polymer absorbs ca. 40 percent water by weight. Finally, on a per equivalent weight basis, the water contents of the Dow PFSI's are significantly lower than the water contents of the Nafion PFSI's (4); this is attributable to the lower crystallinity of the Nafion PFSI's (Figure 2).

Small-Angle X-Ray Scattering. Hydrated Nafion show a SAXS scattering maximum at $Q = 0.15\ A^{-1}$ (18,30). Since the intensity and position of this maximum varied with membrane water content and counterion, this peak was attributed to scattering from the ionic clusters (18,30). Nafion shows a second, less intense, scattering maximum at $Q = 0.05\ A^{-1}$. This maximum, which is observed as a shoulder on the ionic cluster scattering peak, has been attributed to scattering from the Nafion crystallites (17,18,30,31).

The high EW Dow PFSI's also show two scattering maxima (Figure 5). The low Q maxima (ca. $0.05\ A^{-1}$) occur at the same position as the crystalline scattering maxima in Nafion (17,18,31). In agreement with the WAXD and DSC studies, these data demonstrate that the high EW Dow PFSI's are semicrystalline. The intensity and position of the high Q peaks vary with EW and water content; therefore, these maxima are attributed to scattering from the ionic clusters. The data in Figure 5 indicate that all five EW's of the Dow polymers contain ionic clusters.

In general, the intensities of the ionic cluster scattering peaks decrease with increasing EW (Figure 5). An identical trend was observed for Nafion and was attributed to the effect of EW on membrane water content (18,31). As EW increases, water content decreases and the electron-density contrast between the ionic clusters and the fluorocarbon matrix decreases

(31). This decrease in scattering contrast causes the intensity of the SAXS signal to decrease with increasing EW (Figure 5).

A decrease in scattering intensity occurs when the volume fraction of the ionic phase exceeds the volume fraction of the matrix phase (32). The SAXS scan for the 635 EW PFSI demonstrates this effect. Since the 635 EW PFSI imbibes over 180 percent water (Figure 4), the intensity of the ionic scattering peak for this polymer is diminished relative to the 803 EW PFSI.

The electron density contrast in a PFSI can be increased by incorporating an electron-dense metal ion (18,30). Gierke et al. used this approach to obtain SAXS data for dry, Ag^+-form 1200 EW Nafion (18). Figure 6 shows SAXS data for the dry Ag^+-form Dow PFSI's. Scattering maxima are observed for all five EW's. These data indicate that ionic clusters are present in the dry Dow PFSI membranes. We are not at this time sure why the crytalline scattering peaks in Figure 6 have such low intensities. We are currently exploring this point further.

The position of a SAXS peak is defined by the Q value associated with the peak maximum (Q_{max}). Q_{max} values for the ionic domain scattering peaks from the Na^+-form PFSI's are shown in Table III. Bragg spacings calculated from these Q_{max} values are also shown in Table III. If a reasonable scattering model is available, the dimensions of the ionic clusters can be obtained from these data. SAXS data from Nafion have been shown to be quantitatively consistent with a model which assumes that the ionic clusters are a collection of hard spheres dispersed in the polymeric matrix (33).

Assuming that the hard-sphere model (33) applies here, Table III suggests that the diameters of the ionic clusters in the Dow PFSI's decrease with increasing EW. An analogous trend was observed for Nafion (18,33).

The data in Table III also suggest that the ionic clusters in the 635 EW PFSI are much larger than the ionic clusters in the higher EW polymers. This dramatic increase in cluster size correlates well with the dramatic increase in water content for the 635 EW polymer (Figure 4). It is important to note that all of the experimental methodologies tell the same story about the supermolecular structure of the 635 EW Dow PFSI.

Dissolution of the Dow PFSI's. Table I lists conditions suitable for preparing 1 (w/v) percent solutions of the Dow PFSI's. The higher EW polymers required dissolution times of ca. 3 hours; shorter dissolution times yielded large fractions of undissolved polymer. In contrast, 1100 EW Nafion dissolves in one hour (16). This difference in dissolution time undoubtedly reflects the time required to swell the PFSI membrane. Prior to dissolution, solvent molecules must diffuse into the polymer membrane to produce a highly swollen gel. Since the Dow PFSI's are more crystalline than Nafion, longer times are required to form this gel.

PFSI's dissolve when the temperature of the solvent approaches the melting point of the polymer (16). However, solvent molecules incorporated prior to dissolution depress the crystalline melting point. Thus, the dissolution temperature may be significantly lower than the T_m obtained from a DSC experiment (27). Accordingly, the Dow PFSI's are soluble at temperatures below the T_m's listed in Table II.

The 1076 EW and 1269 EW polymers required dissolution temperatures in excess of 250° C; this may be explained via the block-type model discussed above. We propose that the high EW polymers contain small fractions of very long tetrafluoroethylene blocks which organize into thick crystals. Because these thick crystals melt at higher temperatures than the average T_m of the

PFSI, the high EW polymers require elevated dissolution temperatures. Note that because DSC is a rather insensitive technique, endotherms associated with the melting of these small fractions of thick crystals are not observed in the PFSI thermograms (Figure 3).

The 1269 EW PFSI would not dissolve in ethanol/water. Solvent swelling studies yielded an alternative solvent system. While exposure of the 1269 EW polymer to ethanol-water caused the volume of the membrane to increase by 51 percent, 1-propanol-water caused the membrane volume to increase by 77 percent. Because of this enhanced solvent swelling, 1-propanol/water will completely dissolve the 1269 EW polymer (Table I). Thus, dissolution procedures have been developed for all of the Dow PFSI's.

Effect of EW on the Solubility of Solution-Cast Films. The solubilities (in room temperature ethanol/water) of the solution-cast PFSI films decreased as the temperature used during film formation increased (Figure 7). An analogous trend was observed for Nafion (15). We have attributed this temperature dependence to the effects of thermal and solvation energies on polymer chain mobility during film formation (15).

Figure 7 shows that the temperature required to produce highly insoluble films increases with EW. We believe that this trend is attributable to the fact that high EW PFSI's do not form true solutions. Aldebert et al. have shown that PFSI "solutions" contain micelle-like particles (34). The tetrafluoroethylene chains form the core of these particles and the $-SO_3^-$ sites are turned outward to the alcohol-water solution (34).

The size of the micelle formed by a conventional surfactant increases with the length of the hydrophobic chain in the surfactant molecule (35).

We propose that an analogous effect occurs in the Dow PFSI's. Since the lengths of the hydrophobic tetrafluoroethylene segments in a PFSI increases with EW, we propose that the size of the PFSI particle in solution also increases with EW. Thus, larger particles are present in solutions of the high EW polymers and higher thermal energies are required to break up these larger particles. Therefore, higher temperatures are required to yield high-quality (vide infra) solution-cast films of the high EW polymers.

In contrast to the other PFSI's, temperature has little effect on the solubility of the solution-cast 635 EW polymer. The high charge density on this polymer (1 $-SO_3^-$ per every 3.6 tetrafluoroethylenes) may allow true dissolution of the individual polymer chains. Because true solutions are formed, thermal energy is not needed to break up polymer aggregates, and solubility is independent of film-casting temperature (Figure 7).

Solution-Processing. The higher EW versions of the as-received Dow PFSI membranes are strong yet pliant and are insoluble in all solvents at temperatures below ca. 250° C. We have recently found that solution-cast PFSI films which are less than 5 percent soluble (in ethanol/water) retain these desirable characteristics (15). We have called these high-quality solution-cast films "solution-processed" PFSI (15). Solution-cast films which are greater than ca. 5 percent soluble are usually mechanically fragile and disintegrate or dissolve in room temperature ethanol/water.

As indicated in Figure 7, the temperature required to produce highly insoluble, solution-cast Dow PFSI films varied dramatically with EW. The intent of the experiments described in this final section of this paper was to identify solvents and temperatures which yielded high-quality, "solution-processed," films of these polymers. High-quality, solution-processed films

of the 803, 909 and 1076 EW polymers can be prepared by evaporating DMSO to dryness at 185° C (see experimental section and Figure 7).

High quality solution-cast films of the 635 and 1269 EW polymers cannot be obtained from DMSO solutions (Figure 7). Since the as-received 635 EW polymer is ca. 15 percent soluble at room temperature, it is not surprising that the solubility of solution-cast film never drops below ca. 18 percent (Figure 7). Because this polymer is noncrystalline, it is probably impossible to obtain 635 EW films which are highly insoluble.

In contrast to the 635 EW polymer, it seemed likely that higher evaporation temperatures or better cosolvents might yield a high quality solution-processed form of the 1269 EW polymer. We first attempted to use triethylphosphate evaporated at 185° C. These conditions yielded 1269 EW films which were 10 percent soluble, an improvement over DMSO but still too soluble. However, propylene carbonate evaporated at 235° C yielded 1269 EW films which were less than 1 percent soluble. These studies corroborate our earlier conclusion that both solvation and thermal energies are required to yield highly insoluble films (15).

CONCLUSIONS

The new Dow PFSI's (2,4) are structurally and morphologically similar to Nafion. In the 635 to 1269 EW range, the Dow PFSI's contain ionic clusters. EW's above 800 g/mole are semicrystalline and the extent of crystallinity increases with EW. Since the crystalline regions act as barriers to solvent swelling (16), water uptake increases as the extent of crystallinity decreases.

DSC analyses of the Dow PFSI's have shown that the melting points of these polymers vary only slightly with EW. This behavior contradicts the

predictions of theories developed for random copolymers (28). We have proposed a block-type model (29) for the molecular structure of the Dow PFSI's. This model assumes that the crystalline regions are formed from long tetrafluoroethylene blocks.

As noted in the introduction, we are pursuing possible fuel cell appliations for these polymers. Preliminary results of these investiagtions have been reported (14).

ACKNOWLEDGEMENT

We thank Dr. J.S. Lin of the Oak Ridge National Laboratory NCSASR for his kind assistance in obtaining the SAXS data and the Oak Ridge Associated Universities for travel support. Support for this work was provided by the Office of Naval Research, the Electric Power Research Institute and the Center for Space Power at Texas A&M University (sponsored by NASA).

LITERATURE CITED

(1) Eisenberg, A.; Yeager, H.L., Eds. "Perfluorinated Ionomer Membranes," ACS Symposium Series 180, ACS, Washington, D.C., 1982.

(2) Dow Chemical; US Patent # 4,417,969, 1983.

(3) Grot, W. Chem. Ing. Tech. 1978, 50, 299.

(4) Ezzell, B.R.; Carl, W.P.; Mod, W.A., In "Industrial Membrane Processes," White, R.E.; Pintauro, P.N., Eds., AIChE Symposium Series 248, Volume 82, AIChE, New York, 1986.

(5) LaConti, A.B.; Fragala, A.R.; Boyack, J.R. Proc. Electrochem. Soc. 1977, 77, 354.

(6) Yeo, R.S.; McBreen, J.; Kissel, G.; Kulesa, F.; Srinivasan, S. J. Appl. Electrochem. 1980, 10, 741.

(7) Szentirmay, M.N.; Martin, C.R. Anal. Chem. 1984, 56, 1898.

(8) Martin, C.R.; Dollard, K.A. J. Electroanal. Chem. 1983, 159, 127.

(9) Martin, C.R.; Rubinstein, I.; Bard, A.J. J. Am. Chem. Soc. 1982, 104, 4817.

(10) Nagy, G.; Gerhardt, G.A.; Oke, A.F.; Rice, M.E.; Adams, R.A.; Moore, R.B.,III; Szentirmay, M.N.; Martin, C.R. J. Electroanal. Chem. 1985, 188, 85.

(11) Oyama, N.; Ohsaka, T.; Sato, K.; Yamamoto, H. Anal. Chem. 1983, 55, 1429.

(12) Buttry, D.A.; Anson, F.C. J. Am. Chem. Soc. 1983, 105, 685.

(13) Lawson, D.R.; Whiteley. L.D., Martin, C.R.; Szentirmay, M.N.; Song, J.I. J. Electrochem. Soc. 1988, 135, 1988.

(14) Martin, C.R.; Whiteley, L.D.; Lawson, D.R.; Szentirmay, M.N. Polym. Preprnt. 1988, 29(2), 442.

(15) Moore, R.B.,III; Martin, C.R. Macromolecules 1988, 21, 1334.

(16) Martin, C.R.; Rhoades, T.A.; Ferguson, J.A. Anal. Chem. 1982, 54, 1639.

(17) Hashimoto, T.; Fujimura, M.; Kawai, H., In "Perfluoronated Ionomer Membranes," Eisenberg, A.; Yeager, H.L., Eds., ACS Symposium Series 180, ACS, Washington, D.C., 1982, Chapter 11.

(18) Gierke, T.D.; Munn, G.E.; Wilson, F.C. J. Polym. Sci.: Polym. Phys. Ed. 1981, 19, 1687.

(19) Starkweather, H.W., Jr. Macromolecules 1982, 15, 320.

(20) Kyu, T.; Eisenberg, A., In "Perfluoronated Ionomer Membranes," Eisenberg, A.; Yeager, H.L., Eds., ACS Symposium Series 180, ACS, Washington, D.C., 1982, Chapter 6.

(21) Kyu, T.; Hashiyama, M.; Eisenberg, A. Can. J. Chem. 1983, 61, 680.

(22) Eisenberg, A., In "Physical Properties of Polymers," Mark, J.E.; Eisenberg, A.; Graessley, W.W.; Mandelkern, L.; Koenig, J.L., Eds., ACS, Washington, D.C., 1984, Chapter 2.

(23) Gauthier, S.; Duchesne, D.; Eisenberg, A. Macromolecules 1987, 20, 753.

(24) Clas, S.-D.; Eisenberg, A. Polym. Prepn. 1984, 25, 111.

(25) Hodge, I.M.; Eisenberg, A. Macromolecules 1978, 11, 289.

(26) Bassett, D.C.; Davitt, R. Polymer 1974, 15, 721.

(27) Billmeyer, F.W., Jr. "Textbook of Polymer Science," 3rd Edition, John Wiley & Sons, New York, 1984.

(28) Flory, P.J. "Principles of Polymer Chemistry," Cornell University Press, Ithaca, NY, 1953.

(29) Okuda, K. J. Polym. Sci., Part A 1964, 2, 1749.

(30) Fujimura, M.; Hashimoto, T.; Kawai, H. Macromolecules 1981, 14, 1309.

(31) Rodmacq, B.; Coey, J.M.; Escoubes, M.; Roche, E.; Dupplessix, R.; Eisenberg, A.; Pineri, M., In "Water in Polymers," Rowland, S.P., Ed., ACS Symposium Series 127, ACS, Washington, D.C., 1980, Chapter 29.

(32) Kyu, T., In "Materials Science of Synthetic Membranes," Lloyd, D.R., Ed., ACS Symposium Series 269, ACS, Washington, D.C., 1985, Chapter 18.

(33) Kumar, S.; Pineri, M. J. Polym. Sci., Polym. Phys. Ed. 1986, 24, 1767.

(34) Aldebert, P.; Dreyfus, B.; Pineri, M. Macromolecules 1986, 19, 2651.

(35) Missel, P.J.; Mazer, N.P.; Benedek, G.B.; Carey, M.C. J. Phys. Chem. 1983, 87, 1264.

Table I. Dissolution Conditions for the Na^+-Form Dow PFSI's.

EW	Time	Temperature	Solvent
635	1 hour	250°C	ethanol-water
803	3 hours	250°C	ethanol-water
909	3 hours	250°C	ethanol-water
1076	3 hours	275°C	ethanol-water
1269	3 hours	300°C	1-propanol-water

Table II. Effect of equivalent weight on the matrix glass transition temperature ($T_{g,m}$), the ionic cluster glass transition temperature ($T_{g,c}$), and the crystalline melting point (T_m).

EW	$T_{g,m}$ (°C)	$T_{g,c}$ (°C)	T_m (°C)
635	177	297	---
803	179	288	335
909	165	284	336
1076	158	286	338
1269	158	275	338

Table III. SAXS Q_{max}'s and Bragg spacings for the Na^+-form PFSI's.

EW	Q_{max}	*d* (A)
635	0.081	77
803	0.135	46
909	0.147	43
1076	0.154	41
1269	0.159	39

FIGURE CAPTIONS

Figure 1. WAXD scans of (A) 635 EW, (B) 803 EW, (C) 909 EW, (D) 1076 EW and (E) 1269 EW Dow PFSI's. All samples were dry Na^+-form.

Figure 2. WAXD scans of (A) 1100 EW Nafion, (B) 909 EW Dow PFSI and (C) 1076 EW Dow PFSI. All samples were dry Na^+-form.

Figure 3. DSC thermograms of (A) 635 EW, (B) 803 EW, (C) 909 EW, (D) 1076 EW and (E) 1269 EW Dow PFSI's. All samples were dry Na^+-form.

Figure 4. Plot of percent water uptake versus equivalent weight for the Dow PFSI's. All samples were Na^+-form and boiled in water for 1 hour.

Figure 5. SAXS scans of (○) 635 EW, (△) 803 EW, (□) 909 EW, (▽) 1076 EW and (◇) 1269 EW Dow PFSI's. All samples were hydrated Na^+-form.

Figure 6. SAXS scans of (○) 635 EW, (△) 803 EW, (□) 909 EW, (▽) 1076 EW and (◇) 1269 EW Dow PFSI's. All samples were dry Ag^+-form.

Figure 7. Solubilities of solution-cast Dow PFSI's in DMSO as a function of the solvent evaporation temperature: (●) 635 EW; (▲) 803 EW; (■) 909 EW; (▼) 1076 EW; (◆) 1269 EW.

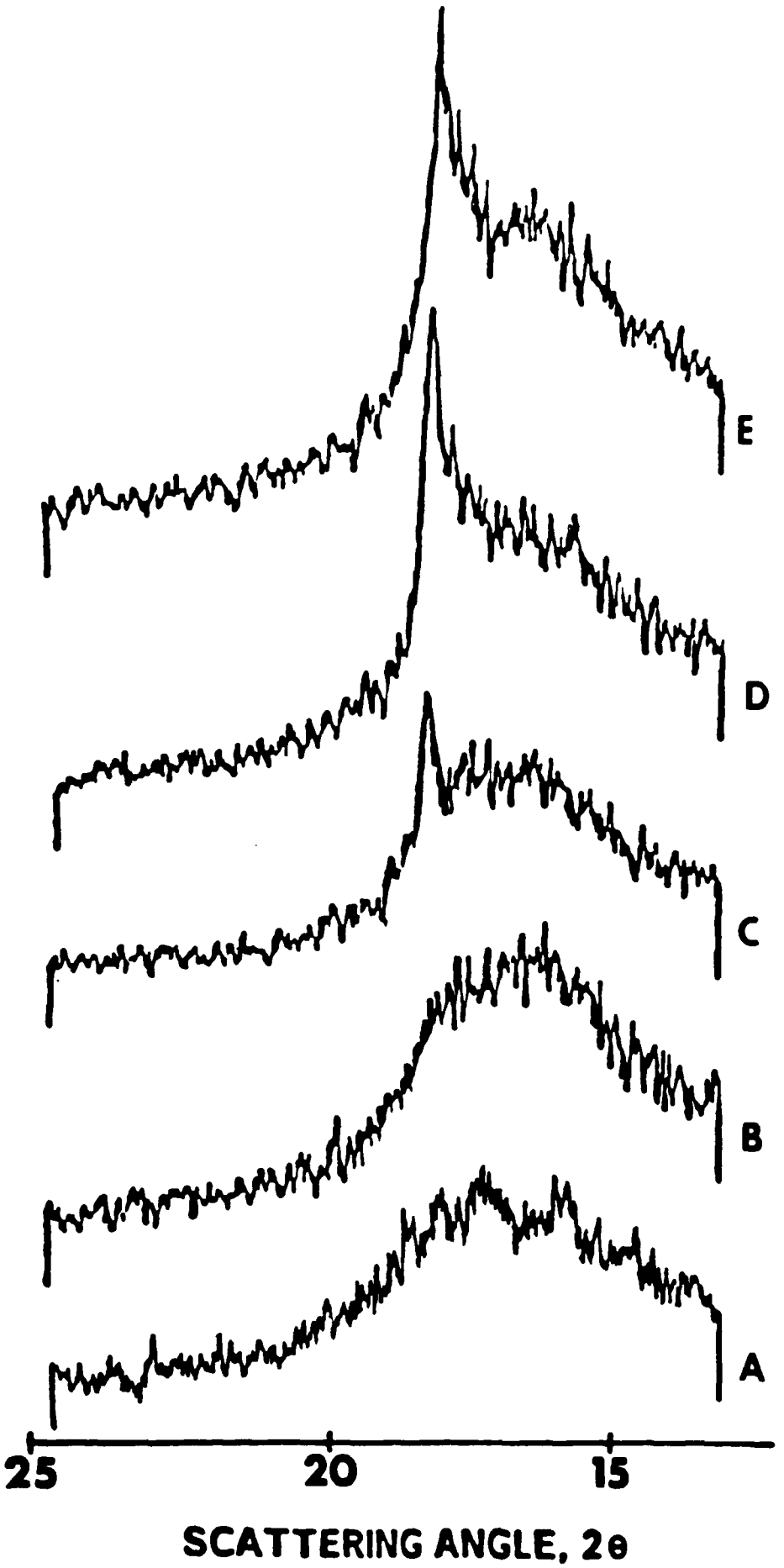

Fig

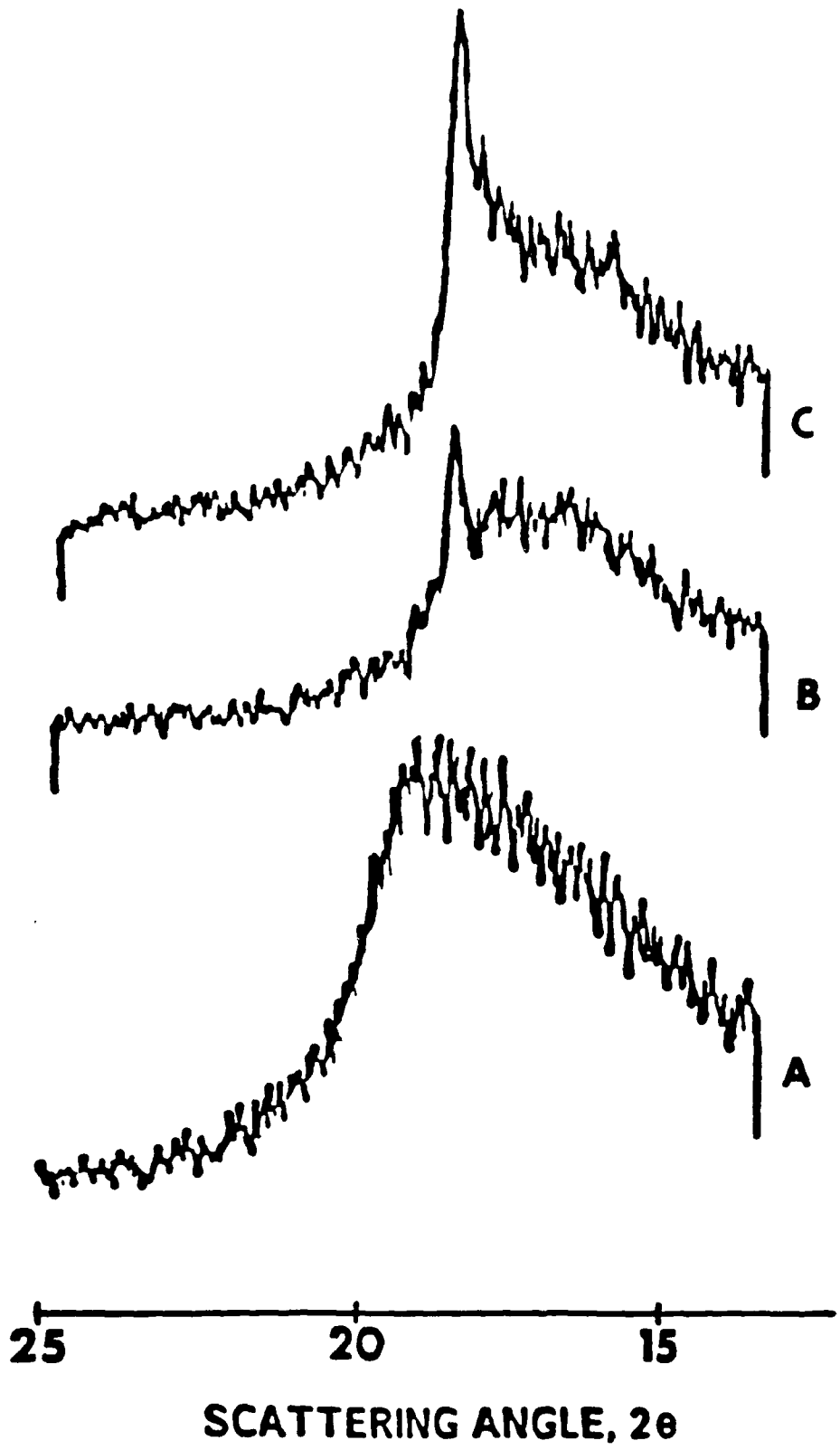

Fig 2

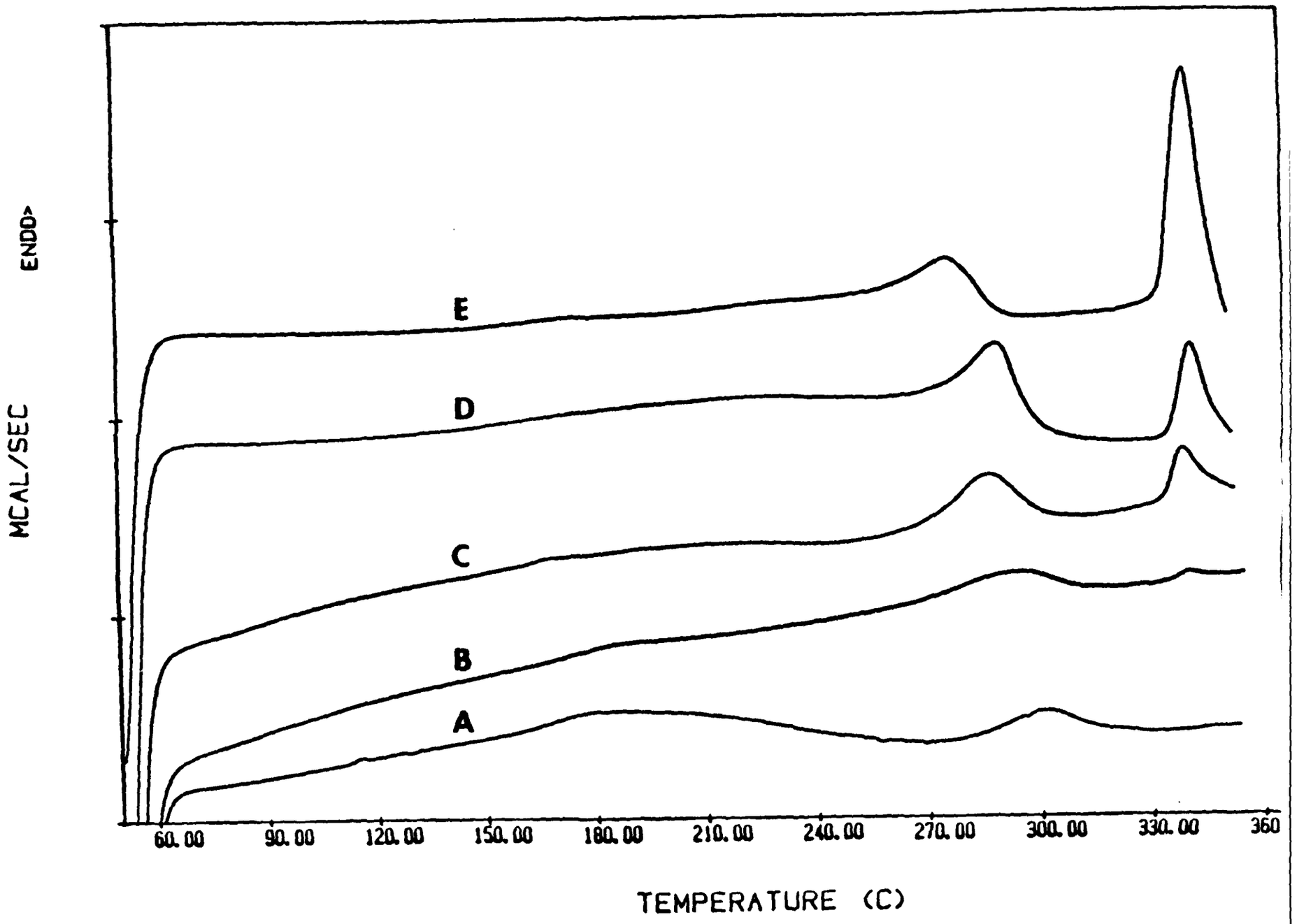
ENDO>
MCAL/SEC
E
D
C
B
A
60.00
90.00
120.00
150.00
180.00
210.00
240.00
270.00
300.00
330.00
360
TEMPERATURE (C)

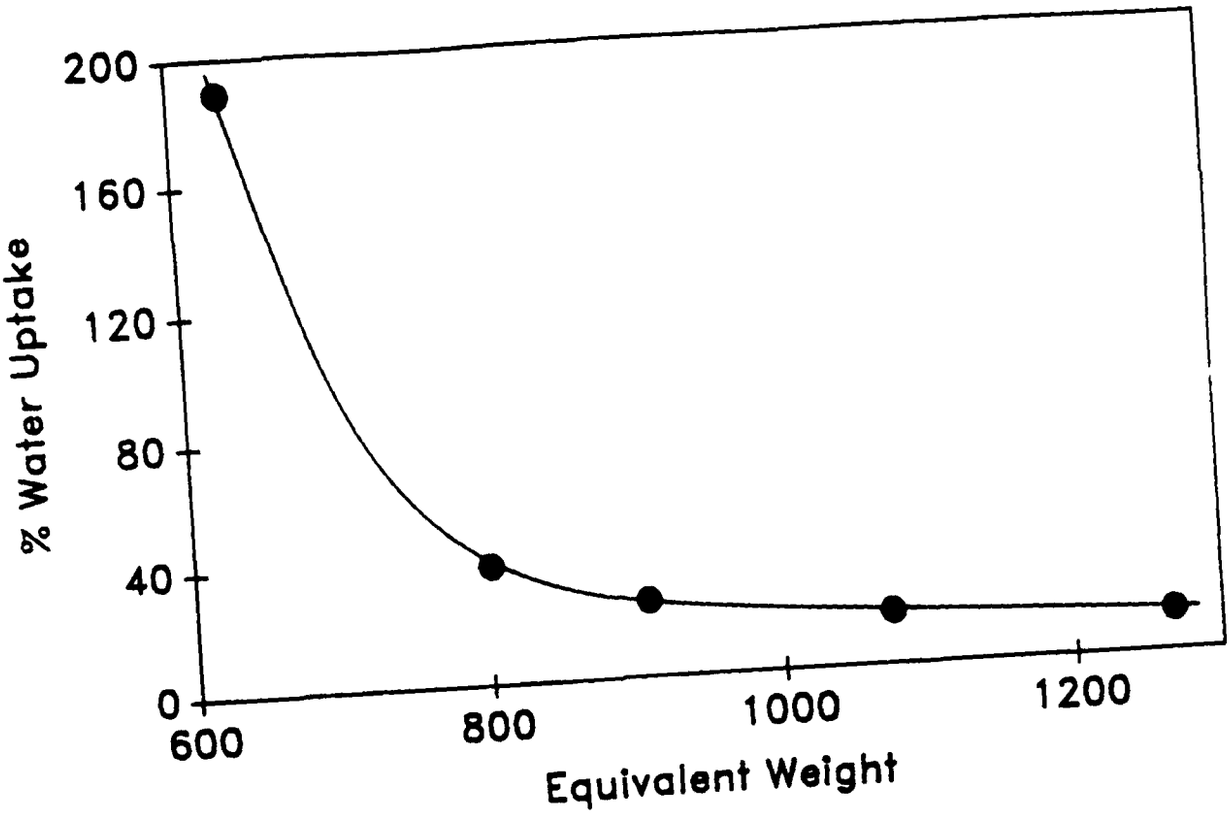
200
160
120
80
40
0
% Water Uptake
600
800
1000
1200
Equivalent Weight

Fig-4

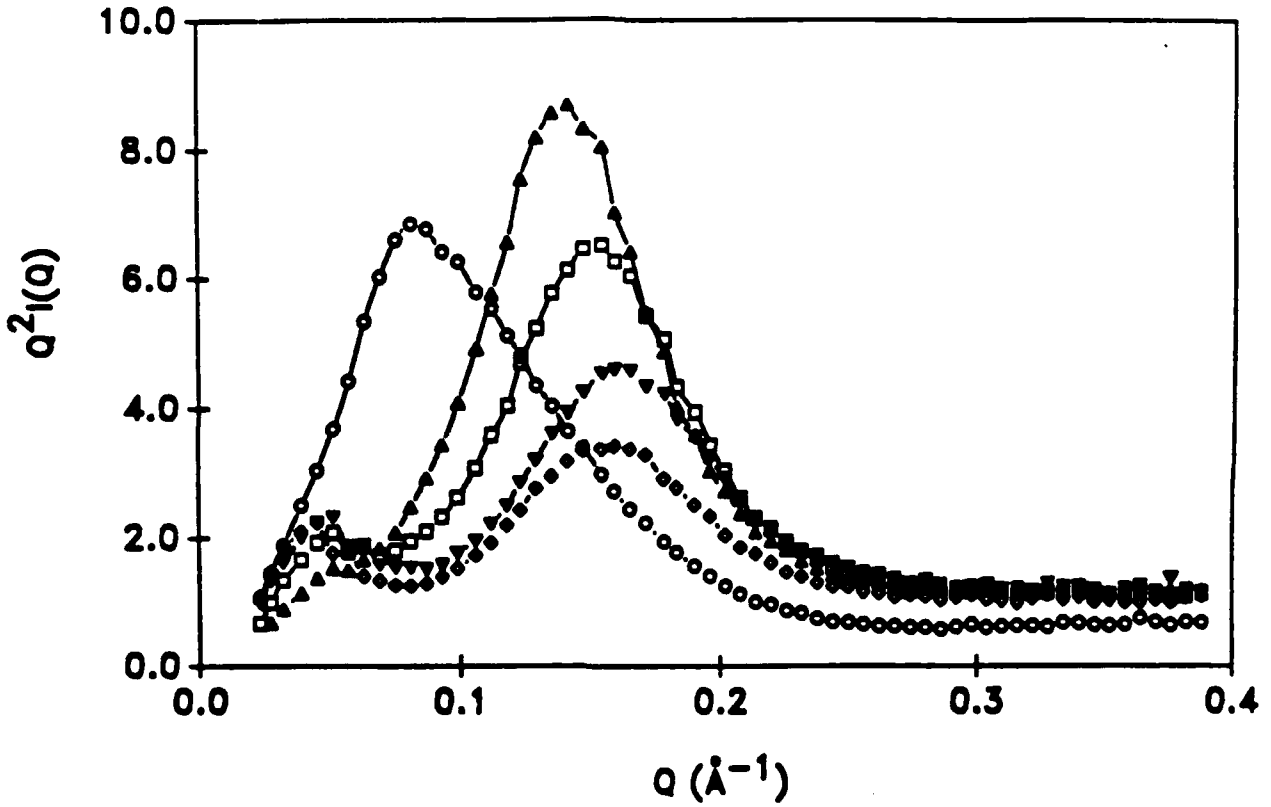

Figure 5

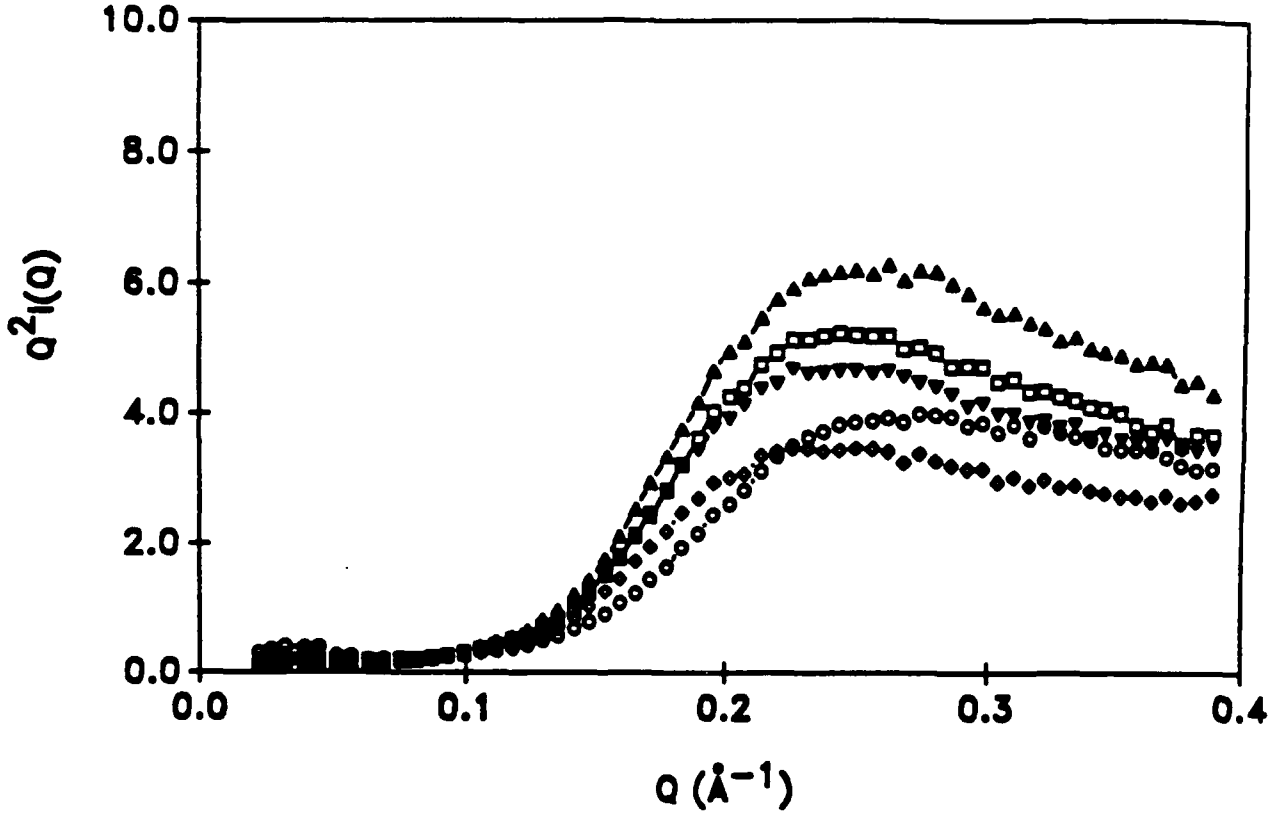

Figure 6

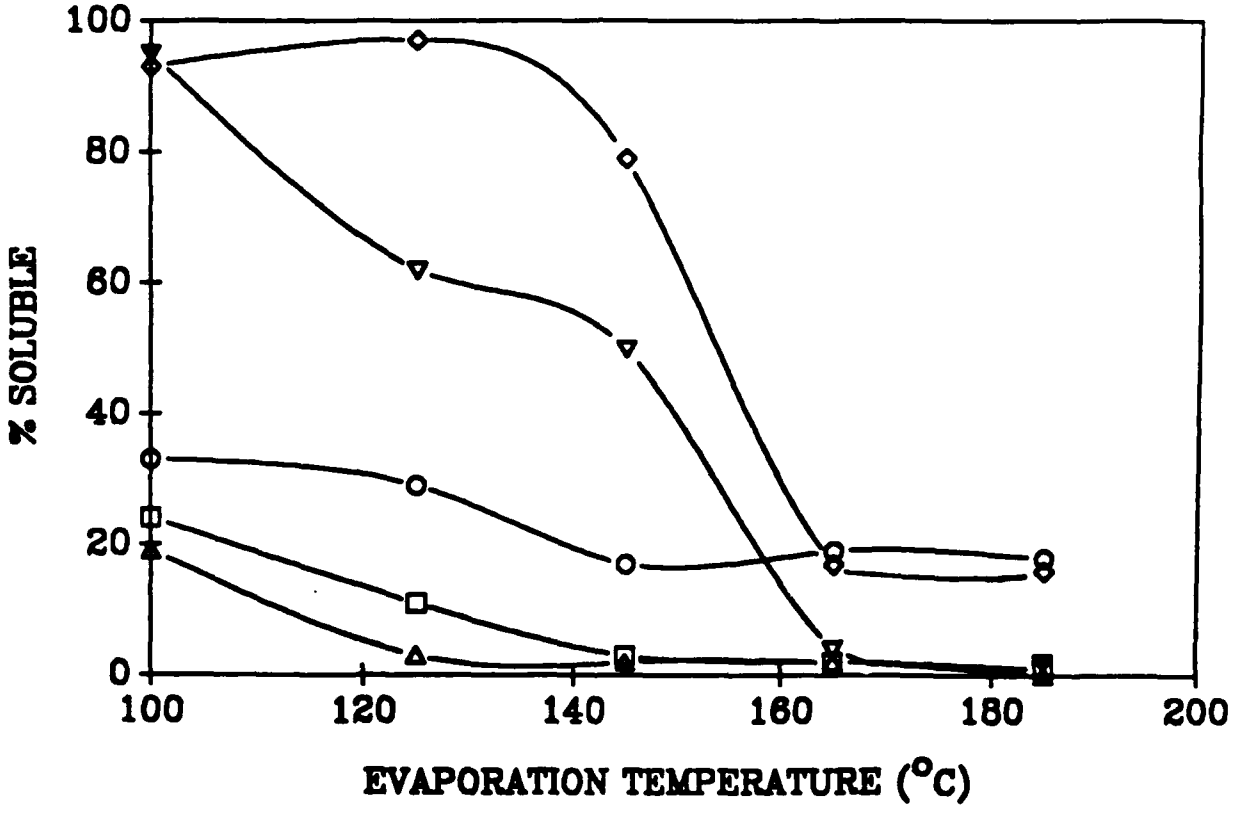
100
80
60
40
20
0
% SOLUBLE
100
120
140
160
180
200
EVAPORATION TEMPERATURE (°C)

END
FILMED
6-89
DTIC